Self-healing UV curable coatings for wood substrates

Chloé PAQUET[a], Jean-François MORIN[b], Véronic LANDRY[c]

a) Département de sciences du bois et de la forêt, Université Laval, Québec
b) Département de chimie et Centre de Recherche sur les Matériaux Avancés (CERMA), Université Laval, Québec
c) Département de sciences du bois et de la forêt, Université Laval, Québec. Holder of the industrial research chair NSERC – Canlak of finishing for interior wood products

Introduction

Abrasion and scratch resistance are amongst the most important properties for interior wood products. To protect wood, UV curable acrylate coatings are used because of their high reactivity that ensures high factory productivity. Despite the good performance of UV curable acrylate coatings, scratches formation is unavoidable as wood is a soft substrate. To ensure scratch repair, extrinsic (vascular and capsules based) and intrinsic self-healing technologies were developed[1].

Extrinsic technology consists of capsules dispersion or capillaries network inside the material. These capillaries and capsules contain a self-healing agent that is released in the scratch after mechanical aggression. Extrinsic technology is totally autonomous but not repeatable.

Intrinsic technology designates materials with reversible bonds, which create a temporary network. This reversibility, with or without external stimuli, is used to enable material repair[1]. In contrast to the extrinsic technologies, intrinsic ones are repeatable but not autonomous. Reversible bonds can be carbon covalent bonds in Diels-Alder reaction, hydrogen bonds, interactions or molecular tangles[1]. During stress, the energy breaks the reversible bond network. Chain mobility allows reversible network to rebind. In some cases, external stimuli are needed to generate this mobility. Diels-Alder reaction creates covalent bonds between diene and dienophile groups. This reaction occurs at room temperature and retro Diels-Alder upon heating[2]. Wudl F. *et al*.[3] used Diels-Alder reaction between furan and maleimide to prepare reversible cross-linked polymers. One of the main observations for Diels-Alder based self-healing materials is that high temperature (100 – 150 °C) is necessary to break covalent bonds. Heating at temperatures higher than 100 °C dries and damages wood[4,5], which makes this technology unappropriated for wood applications. Molecular tangles occur in materials with high chain mobility, namely soft materials[6]. UV curable wood coatings are highly cross-linked, thus tangles technology is not applicable. Concerning weak bonds, bond strength and quantity influence the material hardness[7]. To obtain resistant coatings, one of the strongest non-covalent bond, the hydrogen one, was selected to develop resistant intrinsic self-healing coating for wood applications. Several studies on self-healing system based on hydrogen bonding are presented in the literature. Chen *et al*.[3] developed a polymer with styrene and amide phases. Polyamide phases contain hydrogen bonds ensuring self-healing property. Liu *et al.*[8] used hydrogen bonds in ureido group to prepare oligomers with polyol branches. Stadler *et al.*[9] synthesised several poly(butadiene)s varying hydrogen bonds quantity. They prove that the higher the quantity of hydrogen bonds is, the higher is the temperature needed to generate self-healing. Cortese *et al.*[10] grafted thymine and diaminotriazine on poly(propylene oxide). In this case,

hydrogen bonds quantity depends on thymine and diaminotriazine quantity. This study concludes that increasing hydrogen bonds quantity increases polymer crystallinity[10].

Therefore, increasing hydrogen bonding increase material crystallinity but also the temperature needed to generate self-healing. To obtain resistant coatings for the daily life, it is necessary to have hard polymers. However, to ensure that wood is not damaged during heating, it is important that self-healing occurs at low temperature (under 100 °C). As a result, the challenge is to obtain a UV curable coating resistant ambient conditions that heals under low temperature.

UV curable self-healing coatings are also presented in literature. Wang Z. *et al*.[11] developed UV curable polyurethane which is self-healing. The healing property is based on Diels-Alder reaction and thiol-ene click reaction, and occurs at 90°C. Saman N.M. *et al*.[12] investigated UV curable alkyd coating containing capsules to ensure self-healing behavior. Liu J. *et al*.[13] explored hard core – flexible arm structure. They prepared UV curable polyurethane with hydrogen binding in the flexible part of the material. Thus, hydrogen bond has been used to study UV curable self-healing materials, but only with polyurethane coating. In the case of wood industry, acrylate UV curable coatings are investigated.

The objective of this work was to develop and evaluate intrinsic self-healing formulation applicable to wood industry. Intrinsic technology was selected, and more specifically, hydrogen bond. Formulation of UV-curable acrylate coatings creating hydrogen bond was developed, and their self-healing behavior has been characterized.

Experimental section

Materials

Monomers and oligomers selected are low toxicity acrylates with alcohol or amide groups providing intermolecular hydrogen interactions. Based on preliminary study on mechanical properties, two monomers and two oligomers were selected to test their self-healing behavior. The two monomers with alcohol groups were HEMA and HPPA, presented in Table 1. The two oligomers selected were acrylated allophanate (AA1, AA2) presented in Table 1. The reference coating, without hydrogen bond, was prepared from HDDA and EDA.

Table 1: Components used in coatings formulation

Abbreviation	Name	Viscosity	Supplier	Function
HDDA	1,6-Hexanediol diacrylate	5 cP	Canlak	Monomer
HEMA	2-Hydroxyethyl methacrylate	6 cP	Sigma-Aldrich	Monomer
HPPA	2-Hydroxy-3-phenoxypropyl acrylate	200 cP	Sigma-Aldrich	Monomer
1173	Irgacure 1173: 2-Hydroxy-2-methylpropiophenone	Liquid	Canlak	Photoinitiator absorption peak at 240 nm
AA1	Ebecryl 4738: Aliphatic urethane acrylate, hard resin	35 000 cP	Allnex	acrylated allophanate oligomer
AA2	Ebecryl 4666: Unsaturated aliphatic urethane acrylate, hard resin	56 000 cP	Allnex	acrylated allophanate oligomer
EDA	Epoxy diacrylate resin	30 000 cP	Canlak	epoxy acrylate oligomer

Coating formulation and application procedure

Each formulation was prepared from one monomer, one oligomer and one photoinitiator (1173). The ratio of monomer/oligomer was set to reach a viscosity of 2000 cP. Oligomer, monomer, and photoinitiator were added successively in a metallic flask and stirred with a high-speed disperser (Dissolver DISPERMAT LC30) at 600 rpm. Table 2 presents the formulations composition, the viscosity and the molar functionality. The formulations' molar functionality was calculated using Equation (1)

$$\bar{f} = \frac{f1 * n1 + f2 * n2}{n1 + n2} \quad (1)$$

with f being the functionality and n the moles quantity.

Table 2: Description of the formulation, with the ratio and the viscosity measurements

n°	Monomer	Oligomer	Hydroxyl components	Molar Functionality	Ratio M/O	Viscosity at 5 rpm	Viscosity at 50 cP
1	HDDA	EDA	0	2	17.5/82.5	2315 cP	2486 cP
2	**HEMA**	EDA	1	2	17.5/82.5	2387 cP	2522 cP
3	**HPPA**	EDA	1	1.9	45/55	2267 cP	2408 cP
4	**HEMA**	**AA1**	2	2.9	17.5/82.5	2336 cP	2454 cP
5	**HPPA**	**AA1**	2	2.6	45/55	2188 cP	2254 cP
6	**HEMA**	**AA2**	2	3.9	19/81	2245 cP	2351 cP
7	**HPPA**	**AA2**	2	3.5	50/50	2135 cP	2313 cP

The formulations were applied on several substrates (glass or metallic panel according to tests) with a square applicator film (PA-5353, from BYK) of 100 µm thickness. The films were cured in an

UV oven (ATG 160 305 from Ayotte techno gaz) at 150 mW/cm^2 200 mJ/cm^2. A mercury lamp (UV mac 10 from Nordson) emitting at 200-300 nm was used.

Photo-Differential scanning calorimetry (Photo-DSC)

Photo-DSC was performed with a Mettler Toledo DSC 822e and the LC5 UV mercury spotlight (from Hamamatsu). The lamp intensity was set to 50 mW/cm² with an emission wavelength ranging from 240 nm to 400 nm. 1.9 ± 0.1 mg of each formulation was deposited in open aluminum pan. Samples were irradiated for 1 min. The resulting curve corresponds to the difference of heat flow between the reference (empty pan) and the sample. The measure was performed at constant temperature (30 °C) using the following method: (1) 1 min without irradiation, (2) 1 min with UV light, (3) 2.5 min without irradiation, (4) 1 min with UV light and (5) 0.5 min without irradiation. The first irradiation ensures the photo-polymerisation, the second one was performed to measure the irradiation energy as a blank curve. The second irradiation segment was subtracted from the first one. The integration of the resulting curve was calculated. Then, the conversion was estimated by the StarE software from the integration and the theoretical enthalpy. This last parameter was calculated as described by the Equation (2)

$$\Delta H\ \text{theoretical} = \frac{f_{oligo} * W_{oligo} * \Delta H_{acrylate}}{M_{oligo}} + \frac{f_{mono} * W_{mono} * \Delta H_{acrylate}}{M_{mono}} \quad (2)$$

with f being the functionality, W the weight fraction, M the molar mass, and $\Delta H_{acrylate}$ is 86 kJ/mol[14].

Dynamic mechanical analysis measurements (DMA)

DMA measurements were performed from 30 °C (or 0 °C for low glass transition temperature (T_g) coating) until T_g + 70 °C at 3 °C/min. The parameters selected were the following: 125 % of force track, preload at 0.1 N and 0.2 % of strain. 2.5 x 0.5 cm samples were cut using a CO_2 laser LMC-2000 (laser machine center, from Beam Dynamic). Information obtained by DMA are the loss modulus, the storage modulus and the tan(δ) curves depending on temperature. The maximum of loss modulus represents the T_g. The minimum of storage modulus was used to calculate the cross-linking density following Equation (3)

$$D_c = \frac{E'}{3 * R * T} \quad (3)$$

Where E′ is the storage modulus in the rubbery plateau at T_g + 50 °C, R is the gas constant and T is the temperature at T_g + 50 °C.

Self-healing characterization

Scratch resistance experiments

Coatings were applied on Q-panels R-36. Scratches were performed using a multi-finger scratch/mar tester (Model 710 from Taber Company), using a 10 N weight and a spherico-conical tip of

1 mm radius. The Dektak 150 contact profilometer (from Veeco) was used to measure scratches' depth. Three coatings were prepared from each formulation. Two scratches were prepared on each coating and three profilometer measurements were performed per scratch. Profilometry measurements were realized using a 2.5 µm radius tip and a 1 mg weight. The profilometer measurement was 2 500 µm in length and 20 s in duration. The software was set on "high and valley" profile at a resolution of 524 µm. From the scratch profile (Figure 1), the software measures the scratch depth following Equation (4).

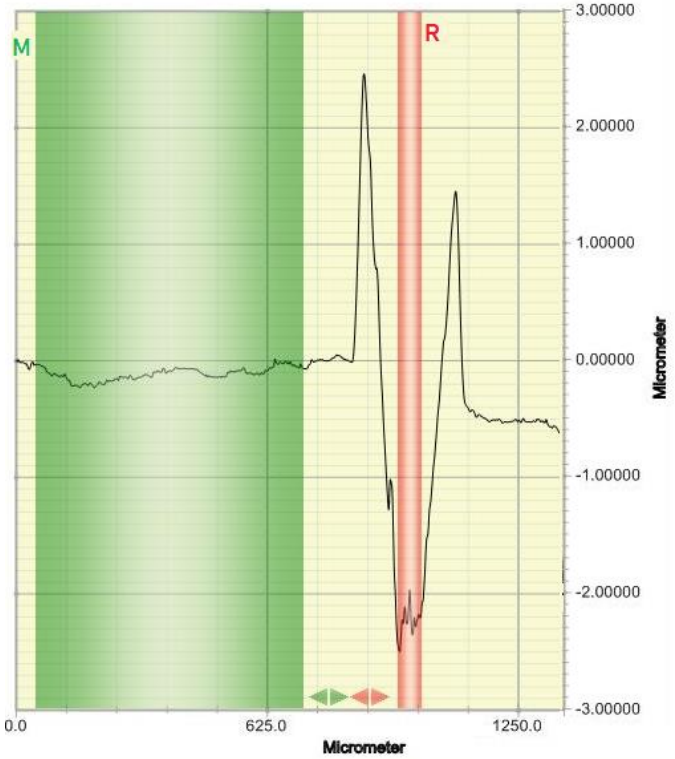

Figure 1: Scratch profile obtain by contact profilometer

$$\text{Scratch depth} = \text{Depth at R point} - \text{depth at M point} \quad (4)$$

Scratch depth before and after healing was used to calculate self-healing efficiency (5). Healing was performed by placing the sample in an oven at 80 °C for 2 h.

$$\text{Self-healing (\%)} = \frac{\text{scratch depth before healing}}{\text{scratch depth after healing}} * 100 \quad (5)$$

Color measurements

As abrasion creates white color on the coating, color measurements were used to characterize self-healing property. Coatings were applied on black glass panels (#3720 from BYK) following the application procedure described previously. Abrasion was performed with the Abrasion and washability tester from Elcometer (#1720), using a scotch Brite hand pad 7447 (from 3M) as abrasion pads. 5 cycles of abrasion were performed at a speed of 37 cycles/min. Then, samples were heated at 80 °C for 2 hrs in the oven. Color measurements were performed before and after abrasion tests and after heating.

Coatings' color was measured using a X-rite Ci6x spectrophotometer. L*, a*, b* values were retrieved from the colorIQ software. The color difference ΔE (before and after healing) was calculated in CIELab system as described in Equation (6):

$$\Delta E = \sqrt{\Delta L^2 + \Delta a^2 + \Delta b^2} \quad (6)$$

Results and discussion

Photo-DSC

The photo-DSC measures the enthalpy of photo-polymerisation to calculate the conversion yield of the acrylate formulation. Table 3 presents the results of photo-DSC measurements.

Table 3: Conversion yield of formulations calculated from the photo-DSC measurement

n°	Formulation	Integration	ΔH theoretical	Conversion
1	HDDA - EDA	0.53	262	33.8 %
2	**HEMA** – EDA	0.46	244	41.3 %
3	**HPPA** - EDA	0.43	249	42.0 %
4	**HEMA – AA1**	0.63	381	41.5 %
5	**HPPA – AA1**	0.61	341	36.0 %
6	**HEMA – AA2**	0.62	347	36.1 %
7	**HPPA – AA2**	0.62	338	34.6 %

Photo-DSC results indicate conversion yields between 35 % and 42 %. These rather low yields can be attributed to the low lamp intensity of 50 mW/cm^2 (the maximum of the lamp), instead of the 150 mW/cm^2 generally used for the irradiation for these acrylate coatings photo-polymerisation. Also, these coatings are the sealer layer, which does not need to be 100% polymerized to ensure good interlayer adhesion. It is notable that the reference coating (n°1) has the lowest conversion yield due to the highly reactive monomer. The higher the formulation reactivity is, the lower is the conversion yield, as the network will cross-link and stiffen faster. For the same reason, the lower the formulation functionality is, the higher is the conversion yield[15]. This explains the high conversion yield of the coatings n°2 and 3, which have functionality of 2 and 1.9, respectively. Conversion yield will be compared with the self-healing results in the following sections.

Dynamic mechanical analysis (DMA)

DMA measurements were used to characterize the T_g of the coatings and their cross-linking density. Results are presented in Table 4

Table 4 T_g and cross-linking density obtained by DMA measurements

n°	Formulation	T_g (°C)	Cross-linking density (mol/m^3)	Functionality
1	HDDA - EDA	43 ± 3	620 ± 108	2
2	**HEMA** – EDA	42 ± 0.5	630 ± 94	2
3	**HPPA** - EDA	37 ± 1	622 ± 42	1.9
4	**HEMA – AA1**	78 ± 2	3268 ± 89	2.9
5	**HPPA – AA1**	55 ± 1	1963 ± 163	2.6
6	**HEMA – AA2**	72 ± 2	3154 ± 124	3.9
7	**HPPA – AA2**	53 ± 3	1801 ± 112	3.5

It is notable that the T_g follows the same pattern as the cross-linking density. The T_g represents the temperature at which the material changes from glass to rubber state. In the glass state, the polymer chains are still, but above the T_g polymeric chains have enough thermal energy to have mobility. High cross-linking implies low chain mobility, which means that more thermal energy is necessary to ensure chain movements. This explains the relation between the T_g and the cross-linking density. For the same reason, high formulation functionality induce high cross-linking density, thus high Tg.

The results indicate that coatings with HEMA monomer and acrylated allophanate oligomers (n°4, 6) have high cross-linking density and T_g values. Also, reference coating HDDA – EDA (n°1) has quite a low T_g and cross-linking density. The results can be explained by the average coating functionality.

Self-healing characterization by scratch depth

Self-healing property was characterized using contact profilometry. Scratch depth before and after healing was measured. The resulting self-healing efficiency is presented in Table 5.

Table 5: Scratch self-healing results measure by contact profilometry

n°	Formulation	Average depth scratch (µm)	Average depth scratch after healing (µm)	Self-healing efficiency (%)
1	HDDA - EDA	1.6 ± 0.8 µm	1.36 ± 0.7 µm	15 ± 3 %
2	**HEMA** – EDA	4.05 ± 2.6 µm	2.22 ± 1.5 µm	45 ± 15 %
3	**HPPA** - EDA	4.4 ± 0.8 µm	3.8 ± 0.6 µm	14 ± 2 %
4	**HEMA – AA1**	1.76 ± 0.1 µm	0.37 ± 0.2 µm	83 ± 11 %
5	**HPPA – AA1**	0.45 ± 0.07 µm	0.37 ± 0.01 µm	18 ± 9 %
6	**HEMA – AA2**	1.15 ± 0.4 µm	0.92 ± 0.4 µm	20 ± 6 %
7	**HPPA – AA2**	0.22 ± 0.04 µm	0.2 ± 0.02 µm	9 ± 1 %

The coating HEMA – AA1 (n°4) presents the highest self-healing efficiency. Also, the coating HEMA – EDA (n°2) shows self-healing property. The coating n°2 has only one component with hydroxyl groups, leading to a low quantity of hydrogen bonds. This explains the lower healing efficiency compared to coating n°4. The reference coating (n°1) does not have reversible bond. The 15% of scratch depth return measured is due to the elastic return. In fact, the heating at 80 °C release elastic stress of the material induced by the scratch. Thus, the low healing efficiency is considered as the elastic part of the stress. It is notable that HPPA monomer and AA2 oligomer do not provide self-healing. This could be due to steric hindrance as HPPA monomer contains an aryl group.

According to this study, two coatings (n°2 and 4) show self-healing behavior. HEMA monomer provide self-healing property. Also, the higher the hydrogen bonds quantity is, the higher is the self-healing efficiency. It is notable that the self-healing coatings are also the ones with the highest conversion. These results have shown that coatings can have enough chain mobility to repair even when they are highly cross-linked.

Self-healing characterization by color measurements

A new method is used to characterize self-healing property. As scratches' formation on transparent coatings leads to whitening (due to light diffusion on roughness), color measurements can be used to measure healing efficiency. If the coating is self-healing, it should normally revert to transparent after heating. ΔE is the color change of the coating after abrasion, before and after heating. Low ΔE means that the coating does not change during heating, so no healing occurs. High ΔE means that the color of the coating change, in this case reverts to transparent. Coatings with high ΔE thus have high self-healing efficiency behavior. The results are presented in Table 6.

Table 6: Self-healing efficiency reported by color measurements

n°	Formulation	Average ΔE
1	HDDA - EDA	0.2 ± 0.01
2	**HEMA** – EDA	0.95 ± 0.05
3	**HPPA** - EDA	0.41 ± 0.18
4	**HEMA – AA1**	0.96 ± 0.17
5	**HPPA – AA1**	0.28 ± 0.16
6	**HEMA – AA2**	0.54 ± 0.20
7	**HPPA – AA2**	0.09 ± 0.03

The coatings HEMA – EDA (n°2) and HEMA – AA1 (n°4) show higher self-healing efficiency. This result coincides with results obtained for the self-healing study on scratch. The values of ΔE are relatively low as the white aspect of abrasion could be due to light scattering on roughness. The color measurement is proceeded without surrounding light, so there is no light scattering. This can explain the low ΔE values. Theoretically ΔE inferior to 1 indicates that the difference between the two colors is not noticeable by the observer. To see the difference between two colors, the value of ΔE has to be superior at 2^{16}.

Conclusion

This paper reports, self-healing UV curable coatings were studied. The challenge was to obtain resistant UV curable coatings with intrinsic self-healing property, applicable to wood industry. Coatings must be highly cross-linked to be resistant but must have enough chain mobility to allow healing. Results indicate that HEMA monomer and AA1 oligomer provide good self-healing behavior as well as good mechanical properties. Also, the quantity of hydrogen bonds impacts the self-healing efficiency. DMA and photo-DSC measurements show that self-healing coatings (n°2 and 4) are highly cross-linked and one of the most polymerized. The innovation of this paper is to present hydrogen based self-healing behavior on UV curable acrylate coatings. Moreover, the healing occurs at 80 °C. In conclusion, this system is self-healing, highly cross-linked and applicable to wood industry as sealer in finish system.

References

1. Blaiszik BJ, Kramer SLB, Olugebefola SC, Moore JS, Sottos NR, White SR. Self-Healing Polymers and Composites. *Annu Rev Mater Res*. 2010;40(1):179-211. doi:10.1146/annurev-matsci-070909-104532

2. Dewar MJS, Pierini AB. Mechanism of the Diels-Alder reaction. Studies of the addition of maleic anhydride to furan and methylfurans. *J Am Chem Soc*. 1984;106(1):203-208. doi:10.1021/ja00313a041

3. Chen X, Dam MA, Ono K, et al. A thermally re-mendable cross-linked polymeric material. *Science*. 2002;295(5560):1698-1702. doi:10.1126/science.1065879

4. White SR, Sottos NR, Geubelle PH, et al. Autonomic healing of polymer composites. *Nature*. 2001;409(6822):794-797. doi:10.1038/35057232

5. Wilson GO, Porter KA, Weissman H, White SR, Sottos NR, Moore JS. Stability of second generation grubbs' alkylidenes to primary amines: Formation of novel ruthenium-amine complexes. *Adv Synth Catal*. 2009;351(11-12):1817-1825. doi:10.1002/adsc.200900134

6. Meng H, Xiao P, Gu J, et al. Self-healable macro-/microscopic shape memory hydrogels based on supramolecular interactions. *Chem Commun*. 2014;50(82):12277-12280. doi:10.1039/C4CC04760E

7. Boyer DB, Chalkley Y, Chan KC. Correlation between strength of bonding to enamel and mechanical properties of dental composites. *J Biomed Mater Res*. 1982;16(6):775-783. doi:10.1002/jbm.820160604

8. Liu R, Yang X, Yuan Y, Liu J, Liu X. Synthesis and properties of UV-curable self-healing oligomer. *Prog Org Coat*. 2016;101:122-129. doi:10.1016/j.porgcoat.2016.08.006

9. Hilger C, Stadler R. Cooperative structure formation by combination of covalent and association chain polymers: 4. Designing functional groups for supramolecular structure formation. *Polymer*. 1991;32(17):3244-3249. doi:10.1016/0032-3861(91)90148-C

10. Cortese J, Soulié-Ziakovic C, Tencé-Girault S, Leibler L. Suppression of Mesoscopic Order by Complementary Interactions in Supramolecular Polymers. *J Am Chem Soc*. 2012;134(8):3671-3674. doi:10.1021/ja2119496

11. Wang Z, Liang H, Yang H, et al. UV-curable self-healing polyurethane coating based on thiol-ene and Diels-Alder double click reactions. *Prog Org Coat*. 2019;137:105282. doi:10.1016/j.porgcoat.2019.105282

12. Saman NM, Ang DT-C, Shahabudin N, Gan SN, Basirun WJ. UV-curable alkyd coating with self-healing ability. *J Coat Technol Res*. 2019;16(2):465-476. doi:10.1007/s11998-018-0124-x

13. Liu J, Cao J, Zhou Z, Liu R, Yuan Y, Liu X. Stiff Self-Healing Coating Based on UV-Curable Polyurethane with a “Hard Core, Flexible Arm” Structure. *ACS Omega*. 2018;3(9):11128-11135. doi:10.1021/acsomega.8b00925

14. Lee TY, Guymon CA, Jönsson ES, Hoyle CE. The effect of monomer structure on oxygen inhibition of (meth)acrylates photopolymerization. *Polymer*. 2004;45(18):6155-6162. doi:10.1016/j.polymer.2004.06.060

15. M. Braithwaite SD. *Chemistry & Technology of Uv & Eb Formulation for Coatings, Inks & Paints, Volume 4: Formulation*. SITA Technology; 1991. https://www.biblio.com/book/chemistry-technology-uv-eb-formulation-coatings/d/1248824156. Accessed February 12, 2020.

16. Mokrzycki W, Tatol M. colour difference ΔE - a survey.October 8, 2012.